

Mathematical Model of Semiconductor Gas Sensor

Shuichi Seto*, Hiroyuki Kawabe¹, Liqin Shi², Yuko Shimomura¹,
Takashi Oyabu³ and Teruaki Katsube⁴

Department of Applied Business Studies, Kinjo College,
1200 Kasama, Hakusan 924-8511, Japan

¹Department of Social Work, Faculty of Social Work, Kinjo University,
1200 Kasama, Hakusan 924-8511, Japan

²Graduate School of Science and Engineering, Saitama University,
255 Shimo-okubo, Sakura, Saitama 338-8570, Japan

³Graduate School of Regional Economic Systems, Kanazawa Seiryō University,
10-1 Ushi, Gosyo, Kanazawa 920-8620, Japan

⁴Department of Information and Computer Sciences, Faculty of Engineering, Saitama University,
255 Shimo-okubo, Sakura, Saitama 338-8570, Japan

(Received September 13, 2004; accepted September 7, 2005)

Key words: gas sensor, simulation, adsorption model

The objective of this study is to simulate physical adsorption on the surface of semiconductor sensors and to develop a method of analyzing qualitatively and quantitatively the chemical species reacting on the surface of semiconductor sensors. In ordinary studies of the detection of gas species by semiconductor sensors, researchers attach importance to the chemical sensitivity of sensors and note the output of sensors in the stationary state in terms of response characteristics. However, the response in the transient state, the region between the beginning of adsorption and the achievement of equilibrium, contains much information about processes of gases adsorbing on the surface of sensors. In this study, we discuss the relationship between the response of a semiconductor sensor and the amount of physically adsorbed gas and construct mathematical models of adsorption on the surface of the sensor. We simulate the signal of a model sensor using an autoregressive model in which the exponential behavior is extracted from the response, and show that gases can be identified and their concentrations can be determined.

1. Introduction

Gas identification is one of the most attractive areas of research in the field of gas sensing. Usually, in the study of gas detection by semiconductor sensors, the selectivity and sensitivity of sensors for specific chemical species, namely, the development and application of sensors to selectively detect a chemical species, are important.^(1,2) However,

*Corresponding author, e-mail address: seto@kinjo.ac.jp

a sensor always returns a response from mixed gases, but sensors that selectively react with specific chemical species have not yet been developed. These problems can be partly solved by introducing many sensors, namely, a sensor array.⁽³⁻⁹⁾ A sensor array is developed to simultaneously detect multiple chemical species, and this makes the detection of specific gaseous chemical species possible by determining the correlation among large amounts of sensor output.

Imagine a physical adsorption of gas molecules on a sensor surface. The transient period, the time between the beginning of adsorption and the attainment of equilibrium, contains significant information about the adsorption of gases onto the surface of the sensor because the adsorption rate and its behavior over time depend on the chemical species and their concentrations in the neighborhood of the surface with respect to the adsorption on the surface. From this view, we developed a new approach of identifying a gas using the integral transformation method.^(10,11) This method is not as analytically precise as the expected result, and it requires a long calculation time to complete the analysis.

The objective of this study is to simulate physical adsorption on the surface of a semiconductor sensor and to provide a method of analyzing qualitatively and quantitatively the chemical species that adsorb on the surface of a semiconductor sensor using an autoregressive (AR) model in which the exponential behavior is extracted from the signal over time, which is widely used in signal processing for purposes such as voice recognition and control. The AR technique is a well-known method for analyzing time-series data.⁽¹²⁻¹⁸⁾ For analyzing gas sensor signals, Derbel et al. described possible techniques of modeling fire detector signals for the design of fire recognition algorithms.⁽¹⁶⁾ Osuna et al. reported a sensor excitation and signal processing approach that combines temperature modulation and transient analysis to enhance the selectivity and sensitivity of metal-oxide gas sensors.⁽¹⁷⁾ Karjalainen et al. reported the estimation of modal decay parameters from noisy measurements of the reverberations of resonating systems.⁽¹⁸⁾

In this study, we first discuss the relationship between the response of a semiconductor sensor and the amount of physically adsorbed gas and construct mathematical models of the adsorption on the surface of the sensor. Second, we simulate the signal of a model sensor using an AR model in which the exponential behavior is extracted from the response. Finally, we show that gases can be identified and their concentrations can be determined.

2. Conductivity of Semiconductor

In the semiconductor gas sensor, electrical conductivity (or resistance) varies with the physical adsorption of gas molecules. We usually detect the change in voltage of a certain part of the circuit in the sensor system. In this section, we discuss the relationship between the electrical conductivity of the semiconductor and the amount of adsorbed molecules.

In the following, we briefly summarize the theory of the electrical conductivity of a semiconductor.⁽¹⁹⁾ In general, the electrical conductivity of a semiconductor, σ , is proportional to the concentration of carrier electrons, n_e :

$$\sigma \propto n_e. \quad (1)$$

The concentration of carrier electrons is related to the band gap, E_g , between the valence band and the conduction band:

$$n_e \propto e^{-\beta E_g}. \quad (2)$$

In the above, $\beta = \frac{1}{k_B T}$, where k_B and T are the Boltzmann constant and the temperature, respectively. Therefore,

$$\sigma = \sigma_c e^{-\beta E_g}, \quad (3)$$

where σ_c is a proportionality constant.

We imagine the adsorption of gas molecules on the surface of a semiconductor. For a small amount of adsorption, the effect of the adsorption on the width of the band gap is so small that we can treat the adsorption as a perturbation of the semiconductor. According to perturbation theory in quantum mechanics,⁽²⁰⁾ the band gap changes as

$$E_g \rightarrow E_g + \varepsilon, \quad (4)$$

and the first order effect, ε , is proportional to the strength of the perturbation. In other words, the number of adsorbed molecules N is

$$\varepsilon = cN, \quad (5)$$

where c is a proportionality constant, the value of which depends on the identity of the adsorbed molecules. Then, the electrical conductivity of the semiconductor with adsorbed molecules, σ_a , becomes

$$\begin{aligned} \sigma_a &= \sigma_c e^{-\beta(E_g + \varepsilon)} \\ &= \sigma_c e^{-\beta E_g} e^{-\beta \varepsilon}, \end{aligned} \quad (6)$$

and therefore the relative change in the electrical conductivity due to adsorption, R_σ , is proportional to the number of adsorbed molecules,

$$\begin{aligned} R_\sigma &= \frac{\sigma_a - \sigma}{\sigma} \\ &= e^{-\beta \varepsilon} - 1 \\ &\approx -\beta \varepsilon \\ &= -c\beta N, \end{aligned} \quad (7)$$

the value of which also depends on the identity of the adsorbed molecules. In the above, we approximate the exponential function in the first order since the perturbation ε is small.

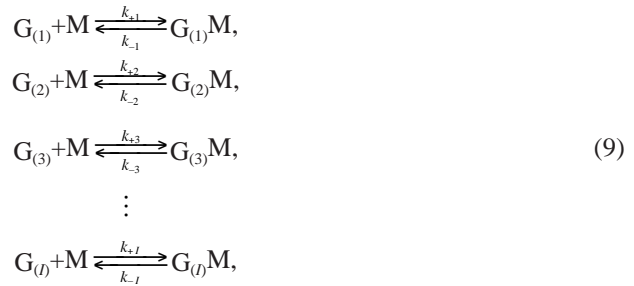
When the number of the adsorbed molecules varies every second, we must define the relative change in the electric conductivity that depends on time $R_o(t)$ as

$$R_o(t) \equiv aN(t), \quad (8)$$

where a is a proportionality constant.

3. Gas Adsorption on Surface of Semiconductor

Consider a physical adsorption process in which a mixed gas composed of I kinds of chemical species $G_{(1)}$, $G_{(2)}$, $G_{(3)}$, ..., $G_{(I)}$ is physically adsorbed on the surface of the semiconductor M , and $G_{(1)}M$, $G_{(2)}M$, $G_{(3)}M$, ..., $G_{(I)}M$ are produced. The adsorption and desorption corresponding to this process are given as



where k_{+i} (k_{-i}) is the adsorption (desorption) rate, $G_{(i)}$ is the surface density of the gas, M is one of the sites available for adsorption, and $G_{(i)}M$ is one of the sites adsorbed.

To simulate the adsorption process, adsorption rate expressions are required. The rate expressions, however, depend on the conditions of the experiments. In measurements of gas detection by semiconductor sensors, we consider two types of experiments: an experiment in a hermetic chamber and one under a flow of gas. In the former, we lead gas into a hermetic chamber, stop the flow of gas, and detect the signal from the sensors. In the latter, fresh gas is continuously introduced during the experiment, and we detect the signal in the existence of the gas flow. We discuss these two cases in the following and show that the relative change in electrical conductivity behaves exponentially in both cases.

3.1 Experiment in hermetic chamber

This is the usual case for physical adsorption. Typical responses of sensors for this case are shown in Fig. 1.

This figure expresses response signals of three sensors in a hermetic chamber for instant noodles. The breath odor measurement was carried out with the following procedures: The base level of each sensor was measured for 30 s and then expiration was introduced into the experimental bottle for 5 s. The three sensor outputs increased after the introduction of the expiration. Usually, the measurement was completed between 60 and 120 min from the beginning of the experiment.

In this model, we introduce the following assumptions. (1) The temperature of the gas

is the same as that of the surface of the sensor. (2) We neglect the diffusion of gas from the surface. (3) We regard the adsorption process on the surface as physical adsorption. (4) The number of sites available for adsorption is much larger than the number of sites that actually adsorb gas during the measurement. (5) This model identifies the species of gas on the basis of the rate of adsorption. (6) We neglect secondary and/or higher-order adsorptions for simplicity.

We find that the curves behave exponentially. In this case, the rate expressions for the adsorption (9) are given as

$$\frac{dG_i(t)}{dt} = -k_{+i}G_i(t)M(t) + k_{-i}N_i(t) \quad (i=1, 2, 3, \dots, I) \quad , \quad (10)$$

$$\frac{dM(t)}{dt} = \sum_{i=1}^I \left\{ -k_{+i}G_i(t)M(t) + k_{-i}N_i(t) \right\} \quad , \quad (11)$$

$$\frac{dN_i(t)}{dt} = -k_{+i}G_i(t)M(t) + k_{-i}N_i(t) \quad (i=1, 2, 3, \dots, I) \quad , \quad (12)$$

where $G_i(t)$, $M(t)$ and $N_i(t)$ are the time-dependent surface densities of $G_{(i)}$, M and $G_{(i)}M$, respectively.

We introduce the dilute gas approximation as

$$\sum_{i=1}^I G_i(t) \ll M(t) \quad . \quad (13)$$

This means that the number of gas molecules in the neighborhood of the surface is so small that the surface of the sensor is not covered with them. As the adsorption proceeds, $G_i(t)$ and $M(t)$ gradually decrease and $N_i(t)$ gradually increases; however, the relative decrease of $M(t)$ is very small. Therefore, $M(t)$ can be approximated to be constant over time:

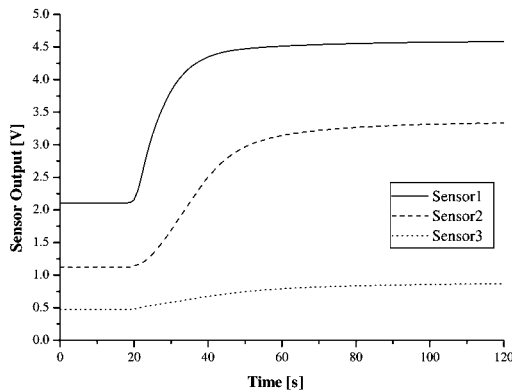


Fig. 1. Responses of sensors to acetone in hermetic chamber. Three typical signals from metal oxide gas sensors (solid line, broken line and dotted line) are shown.

$$\frac{dM(t)}{dt} \approx 0 \quad (14)$$

We then express the adsorption rate equations in the dilute gas approximation as

$$\begin{aligned} \frac{dG_i(t)}{dt} &= -\tilde{k}_{+i}G_i(t) + k_{-i}N_i(t), \\ \frac{dN_i(t)}{dt} &= \tilde{k}_{+i}G_i(t) - k_{-i}N_i(t), \end{aligned} \quad (15)$$

where

$$\tilde{k}_{+i} = Mk_{+i} \quad (16)$$

and M is the initial value of M . We solve the above coupled differential eqs. (15) under the conditions that the initial value of $N_i(t)$ is 0:

$$\begin{aligned} G_i(t) &= G_i \left[1 - \frac{\tilde{k}_{+i}}{\tilde{k}_{+i} + k_{-i}} \left\{ 1 - e^{-(\tilde{k}_{+i} + k_{-i})t} \right\} \right], \\ N_i(t) &= G_i \frac{\tilde{k}_{+i}}{\tilde{k}_{+i} + k_{-i}} \left\{ 1 - e^{-(\tilde{k}_{+i} + k_{-i})t} \right\}, \end{aligned} \quad (17)$$

where G_i is the initial value of $G_{(i)}$. The amplitude of the solution to eq. (17) is proportional to the initial surface density of the gas.

We assume that the gas molecules of each chemical species contribute independently to the relative changes in the electrical conductivity of the sensor. As shown in the previous section, the relative change in the electrical conductivity of the sensor is proportional to the number of adsorbed molecules. Therefore, we have

$$\begin{aligned} R_\sigma &= \sum_{i=1}^I a_i N_i(t) \\ &= \sum_{i=1}^I a_i G_i \frac{\tilde{k}_{+i}}{\tilde{k}_{+i} + k_{-i}} \left\{ 1 - e^{-(\tilde{k}_{+i} + k_{-i})t} \right\} \end{aligned} \quad (18)$$

$$\equiv \sum_{i=1}^I \tilde{G}_i \left(1 - e^{-\tilde{k}_i t} \right), \quad (19)$$

where

$$\tilde{k}_i = Mk_{+i} + k_{-i}, \quad (20)$$

$$\tilde{G}_i = a_i G_i \frac{Mk_{+i}}{Mk_{+i} + k_{-i}}, \quad (21)$$

\tilde{k}_i is the effective adsorption rate constant and is unique for each combination of chemical species in the gas and also to the sensor. \tilde{G}_i is the amplitude of the sensor response for chemical species $G_{(i)}$ and is proportional to the initial surface density of $G_{(i)}$. Equation (19) shows that the relative change in the electrical conductivity of the sensor due to the adsorption of gas tends exponentially toward a stationary value; the chemical species can be identified by the exponent, and its surface density can be determined by the amplitude.

3.2 Experiment under gas flow

Typical responses for this case are shown in Fig. 2. This figure expresses a sensor response signal for the mixed gases in air flow. The current-voltage characteristics of sensor responses were measured by a data acquisition system under repeated gas flows (500 sccm) between NO_2 (diluted in standard air) and standard air (O_2 : 20%, N_2 : 80%) controlled by a mass flow controller (SG-7S1, Aera Japan, Ltd.). The sample was held inside a temperature-controlled electrical furnace at 180°C (ARF-40k, Asahi-Rika Co.).

We find that the signal from mixed gases demonstrates the additivity of the signals and that the curves behave linearly over time when the adsorption is at equilibrium. This behavior results from the flowing gas. Therefore, in this case, we must take into account the gas flow.

We assume that the gas flows with velocity v from minus infinity to infinity along the x axis and that a bulk sensor is placed from 0 to L along the x axis (see Fig. 3). Due to the gas flow, a gradient in the surface density of the gas exists at the sensor because of adsorption. Therefore, we have the following reaction rate equations in the dilute gas approximation:

$$\begin{aligned}\frac{\partial G_i(x,t)}{\partial t} &= -\tilde{k}_{+i} G_i(x,t) + k_{-i} N_i(x,t) - v \frac{\partial G_i(x,t)}{\partial x}, \\ \frac{\partial N_i(x,t)}{\partial t} &= \tilde{k}_{+i} G_i(x,t) - k_{-i} N_i(x,t)\end{aligned}\quad (22)$$

with the boundary conditions

$$G_i(x,0) = \delta(x) G_i, \quad (23)$$

$$G_i(0,t) = G_i \quad (t \geq 0) \quad (24)$$

$$N_i(x,0) = 0 \quad (x \neq 0). \quad (25)$$

Since all the adsorbed molecules contribute to the signal of the sensor, we must integrate the solution of eq. (22) with respect to x as

$$G_i(t) = \int_0^L dx G_i(x,t), \quad (26)$$

$$N_i(t) = \int_0^L dx N_i(x,t), \quad (27)$$

The above coupled partial differential equation, eq. (22), can be solved exactly by the

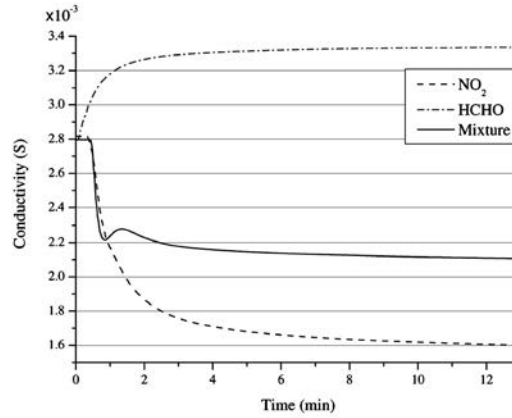


Fig. 2. Response of sensor in gas flow. The broken line, dashed line and solid line correspond to the signals of nitrogen dioxide, formaldehyde and the mixed gas, respectively.

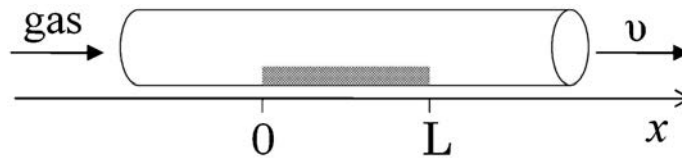


Fig. 3. Semiconductor sensor in tube with flowing gas. The gas flows with velocity v from minus infinity to infinity along the x axis, and a bulk sensor is placed from 0 to L along the x axis.

Laplace transformation. The exact solution is, however, too complex for us to apply to the analysis of the signal of the sensor (see Appendix). Therefore, we approximate the partial differentiation of $G_i(x, t)$ with respect to x and set it constant as

$$\frac{\partial G_i(x, t)}{\partial x} \approx -\frac{\lambda_i G_i}{vL}, \quad (28)$$

where λ_i is a positive definite. We then have an approximated differential equation,

$$\begin{aligned} \frac{dG_i(t)}{dt} &= -\tilde{k}_{+i} G_i(t) + k_{-i} N_i(t) + \lambda_i G_i, \\ \frac{dN_i(t)}{dt} &= \tilde{k}_{+i} G_i(t) - k_{-i} N_i(t), \end{aligned} \quad (29)$$

and obtain the solution with

$$\begin{aligned} G_i(t) &= G_i \frac{\tilde{k}_{+i}}{\tilde{k}_{+i} + k_{-i}} \left[2 + \lambda_i t - \left(1 - \frac{\lambda_i}{\tilde{k}_{+i} + k_{-i}} \right) \left\{ 1 - e^{-(\tilde{k}_{+i} + k_{-i})t} \right\} \right], \\ N_i(t) &= G_i \frac{\tilde{k}_{+i}}{\tilde{k}_{+i} + k_{-i}} \left[\lambda_i t + \left(1 - \frac{\lambda_i}{\tilde{k}_{+i} + k_{-i}} \right) \left\{ 1 - e^{-(\tilde{k}_{+i} + k_{-i})t} \right\} \right]. \end{aligned} \quad (30)$$

Therefore, the relative change in the electrical conductivity becomes

$$R_\sigma(t) = \sum_{i=1}^I \tilde{G}_i \left[\lambda_i t + \left(1 - \frac{\lambda_i}{\tilde{k}_i} \right) \left(1 - e^{-\tilde{k}_i t} \right) \right]. \quad (31)$$

The relative change in the electrical conductivity of the sensor in the flowing gas, eq. (31), is composed of two kinds of terms: a linear term in time, which we have already seen in Fig. 2, and the exponentially saturating term. Removing the linear term in time using the trend-second differentiation with respect to t , and other methods, we have an exponentially saturating or decaying term with an amplitude that is proportional to the surface density of gas:

$$R_\sigma(t) \rightarrow \sum_{i=1}^I \tilde{G}_i \left(1 - \frac{\lambda_i}{\tilde{k}_i} \right) \left(1 - e^{-\tilde{k}_i t} \right), \quad (32)$$

$$\frac{d^2 R_\sigma(t)}{dt^2} = \sum_{i=1}^I \tilde{G}_i \tilde{k}_i^{-2} \left(\frac{\lambda_i}{\tilde{k}_i} - 1 \right) e^{-\tilde{k}_i t}. \quad (33)$$

The behavior expressed in eqs. (32) and (33) is exponential, the same as in eq. (19). Therefore, we can both identify the chemical species and determine its surface density for experiments in flowing gas.

4. Autoregressive (AR) Model

It is important to estimate parameters characterizing the signal using the time series data analysis. However, it is still difficult to build a mathematical model because of the influence of noise. One solution is to adopt the probability process model that is appropriate for the time series data. The AR model is one common method for characterizing the dynamic input-output relationship and is a regression analysis used for the analysis of a time series signal. It is used widely in signal processing for purposes such as voice recognition and control. In the AR model, the parameters describing exponential behavior, namely, the decay constants and the amplitudes, are sought using the least-squares method. Therefore, we analyze the relative change in the electrical conductivity of

the semiconductor sensor with the AR model and reproduce the reaction rate constants and the initial amplitudes.

We express the observed signal as $\{x_n | n = 0, 1, \dots, N-1\}$. The K -th order ordinal AR model is expressed by the following equation:

$$\hat{x}_n = \sum_{m=1}^K a_m x_{n-m}, \quad (34)$$

where \hat{x}_n and a_n are a predicted value and an AR coefficient, respectively. When we estimate the AR coefficient from adjacent data, the predicted values are greatly influenced by noise. In experiments, one ordinal technique to reduce the influence of noise is the repetition of measurement. From the viewpoint of the repetition of a measurement, we divide the signal points into d sets as

$$\begin{array}{rcll} 1 & : & x_0 & x_d & x_{2d} & \cdots & , \\ 2 & : & x_1 & x_{d+1} & x_{2d+1} & \cdots & , \\ 3 & : & x_2 & x_{d+2} & x_{2d+2} & \cdots & , \\ & & \vdots & \vdots & \vdots & & \\ d & : & x_{d-1} & x_{2d-1} & x_{3d-1} & \cdots & , \end{array}$$

and therefore modify eq. (34) and introduce a repetitive number d in the subscript of x as

$$\hat{x}_n = \sum_{m=1}^K a_m x_{n-m \times d}. \quad (35)$$

As a result, we have a set of d AR equations and we solve the combined equation. This means that the time interval of signals in the modified AR model is d times coarser than in the original one, but the measurement is repeated d times.

5. Numerical Simulation

Numerical simulations are performed in order to check the validity of our model and technique. A sensor output model is the sum of three exponential functions, i.e., three chemical species and noise e_n :

$$x_n = \sum_{i=1}^3 C_i \left(1 - e^{-k_i n \Delta t} \right) + e_n. \quad (36)$$

The values of the reaction rate constant k_i and the amplitude C_i are shown in Table 1. The numerical simulations are performed with some noise level e , a sampling time interval Δt (0.025 s), a number of data points N (65536 points), and a repetition number for the measurement d . The repetition number of the measurement d is 1 or 449 (in the case of no noise). The number 449 was determined so that $x_1/x_d = 0.85$.

For the waving signal, the characteristic time is the time of one period of the signal. For the exponential curve, it is the width of the half value. Therefore, we selected d as half of the width of the half value.

If parameter d is small, the estimation error becomes large. If parameter d is large, the

time resolution becomes low.

The noise level was set to 0, 0.001 and 0.01. These were values relative to the initial total amplitude of 4.0000. For example, when $e = 0.01$, we made the uniform random number in the range of ± 0.04 noise. We determined the order of the AR model by the least-squares method.

The results of numerical simulations are shown in Table 2 and Fig. 4. In this table, only the data with large amplitudes are retained. The case of $d = 1$ is equivalent to the traditional AR model. The AR model using our technique ($d = 449$) successfully reproduces the parameters of the sensor output model with sufficient accuracy. On the other hand, with calculations not using our technique ($d = 1$), even for the signal without noise ($e = 0$), it is hard to separate the exponential curves. For signals with noise, the AR model using our technique ($d = 448$ or 449) successfully reproduces the parameters of a sensor output model with sufficient accuracy. Therefore, the idea of the repetition of measurements is essential in order to reduce the influence of noise and to obtain results with sufficient accuracy.

Table 3 shows results of calculations varying the repetition number of measurement d ($\Delta t = 0.025$, $N = 65536$, $e = 0.001$). The influence of noise becomes larger when d is small,

Table 1
Reaction rate constants and initial concentrations.

k_1	C_1	k_2	C_2	k_3	C_3
0.0050	1.0000	0.0100	1.0000	0.0200	2.0000

Table 2

Results of numerical simulations. The numerical simulations are performed with some noise level e , the sampling time interval Δt (0.025 s), the number of data points N (65536 points), and the repetition number of the measurement d . The noise level is set to 0, 0.001 and 0.01. The repetition number of measurement d is 1 or 449 (in the case of no noise). The number 449 was determined so that $x_i/x_{i=0.85}$. The case of $d=1$ is equivalent to the traditional AR model.

noise (e)	d	k_1	C_1	k_2	C_2	k_3	C_3
0	1	0.0060	1.6339	0.0191	2.3661	—	—
0	449	0.0050	1.0000	0.0100	1.0003	0.0200	1.9999
0.0001	1	0.0140	3.7080	6.8148	0.0684	—	—
0.0001	449	0.0050	1.0107	0.0101	1.0089	0.0201	1.9807
0.01	1	0.0448	1.8340	6.6666	0.5476	—	—
0.01	448	0.0051	1.0999	0.0115	1.1849	0.0211	—

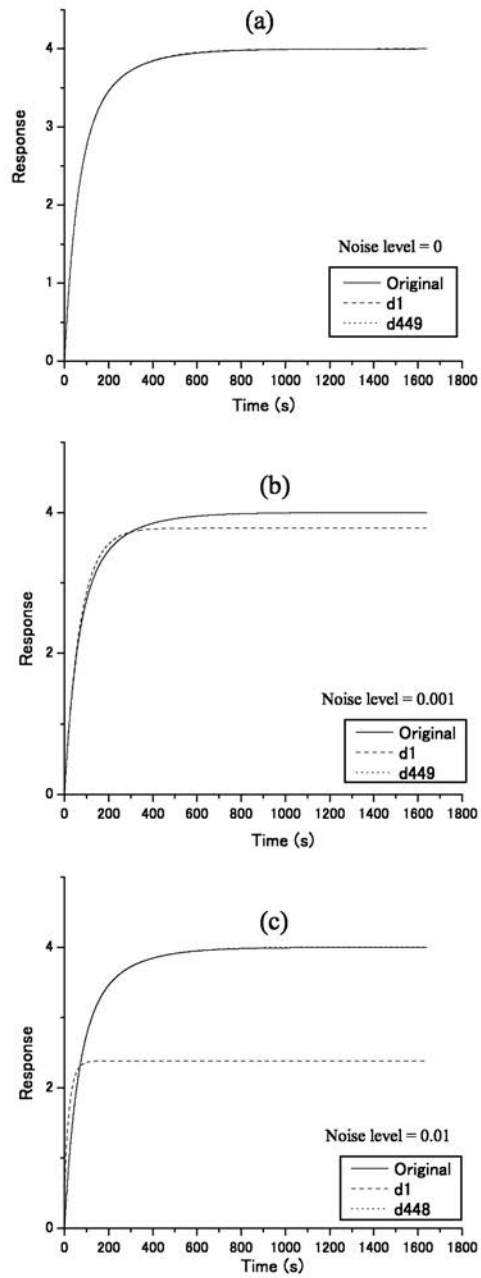


Fig. 4. Simulated responses with different levels of noise and fitted curves. The solid line, broken line and dotted line express the original exponential functions, the fitted curves obtained using the traditional AR model ($d=1$) and the one obtained by our method ($d=449$), respectively. (a) Noise level=0, (b) noise level=0.001 and (c) noise level=0.01.

and the accuracy becomes poor according to the decrease in resolution time when d is too large. It is expected that intermediate d values give good results. For example, a value of d which makes $x_1/x_d \approx 0.85$ may be a good choice.

As a preliminary application of the experimental data, we analyzed the responses of the sensor shown in Fig. 2 using the AR model. The calculated adsorption rate constants and the surface density for NO_2 and HCHO are given in Table 4. Unfortunately, because of a bulge in the curve for mixed gases, we obtained irrational oscillating solutions and could not verify the identification of chemical species and the additivity of the signals.

Table 3

Results of numerical simulations for various d . The numerical simulations are performed with the noise level e (0.001), the sampling time interval Δt (0.025 s), and the number of data points N (65536 points). In this table, only the data with large amplitudes are retained.

$d(x_1/x_d)$	k_1	C_1	k_2	C_2	k_3	C_3
290(0.90)	0.0050	1.0122	0.0101	1.0087	0.0200	1.9796
620(0.80)	0.0050	1.0124	0.0101	1.0106	0.0200	1.9772
1003(0.70)	0.0059	1.3425	0.0159	1.8563	0.0255	0.7898
1460(0.60)	0.0048	0.9107	0.0092	0.9974	0.0197	2.0913
2021(0.50)	0.0050	1.0366	0.0104	1.0537	–	–

Table 4

Calculated reaction rate constants and concentrations for Fig. 2. The calculations are performed with the sampling time interval Δt (0.02 s) and the number of data points N (42400 points). The repetition number of measurement d was determined so that $x_1/x_d = 0.85$.

Gas	k_1	C_1	k_2	C_2
HCHO (600 ppb)	0.028034	0.493381	–	–
NO_2 (300 ppb)	–	–	0.016444	–1.105810
Mixture	0.040600	0.150000	0.010300	–0.799871

6. Concluding Remarks

In this study, we have shown that the relative change in the electrical conductivity of a semiconductor sensor due to adsorption is proportional to the amount of adsorbed molecules and the corresponding proportionality constant depends on the identity of the adsorbed molecule. To the extent that the interaction between the adsorbed molecules is negligible, the additivities of the electrical conductivities of the semiconductor sensor are valid. Therefore, the relative change in the electrical conductivity becomes the sum of the contributions of all the chemical species adsorbed.

We provided two mathematical models of an adsorption on the surface of a sensor: an experiment in a hermetic chamber and one under gas flow. For both models, the relative change in the electrical conductivity of the sensor due to the adsorption of gas tended exponentially toward a stationary value, and the chemical species were identified by the exponents and their surface densities were determined by the amplitudes of the signals.

In order to analyze the time series signal that behaves exponentially, we modified the AR model, introduced the idea of repetitive measurements to reduce the influence of noise, and obtained the exponents and amplitudes with sufficient accuracy.

One problem remaining is to treat a large number of experimental data points and to verify that the mathematical model of the semiconductor sensor and the modified AR model work well.

References

- 1 T. Oyabu, T. Katsube and H. Kimura: *Chemical Sensor System and Soft Computing* (Kaibundo Publishing, Tokyo, 2001).
- 2 Y. Nakamoto, T. Oyabu and H. Kimura: 5th International Conference on Engineering Design and Automation (EDA2001, Las Vegas, 2001) **525** 1110.
- 3 J. W. Gardner: *Microsensors: Principles and Applications* (John Wiley & Sons, New York, 1994).
- 4 K. Toko: *Biomimetic Sensor Technology* (Cambridge University Press, Cambridge, 2000).
- 5 F. Motokizawa: *Aroma Science* (Chuoh Publishing, Tokyo, 1998).
- 6 Y. Kurioka and M. Sotoike: *Applied Engineering of Aroma* (Asakura Publishing, Tokyo, 1997).
- 7 J. D. Winefordner: *Principles of Chemical and Biological Sensors* (John Wiley & Sons, New York, 1998).
- 8 R. Joshi and A. C. Sanderson: *Multisensor Fusion: A Minimal Representation Framework* (World Scientific Publishing, London, 1999).
- 9 G. O. Mutambara: *Decentralized Estimation and Control for Multisensor Systems* (CRC Press LLC, New York, 1998).
- 10 H. Kawabe, S. Seto, Y. Shimomura, T. Oyabu and T. Katsube: *IEEJ Sensors and Micromachines Society, Chemical Sensor* (2002) 35.
- 11 H. Kawabe, S. Seto, Y. Shimomura and T. Oyabu: 6th International Conference on Conference on Engineering Design and Automation (EDA2002, Hawaii, 2002) **6k167** 699.
- 12 M. Hino: *Spectral Analysis* (Asakura Publishing, Tokyo, 2002).
- 13 T. Nakamizo: *Signal Analysis and Identification System* (Corona Publishing, Tokyo, 1988).
- 14 S. Takahashi, T. Shimamura: *Fundamental Digital Signal Processing of One Dimension* (Baifucan, Tokyo, 2001).
- 15 K. Akaike: *Practical Analysis of the Time Series Data* (Asakura Publishing, Tokyo, 2003).
- 16 F. Derbel, M. Horn and H.-R. Trankler: *IMTC99, IEEE Multiconference* (1999).
- 17 R. G.-Osuna, A. G.-Galvez and N. Power: *Sens. and Actuators, B* **93** (2003) 57.
- 18 M. Karjalainen, P. Antsalo, A. Makivirta, T. Peltonen and V. Valimaki: *J. Audio Eng. Soc.* **50** (2002) 867.
- 19 C. Kittel: *Introduction of Solid State Physics* (John Wiley & Sons, New York, 1995).
- 20 L. I. Schiff: *Quantum Mechanics* (McGraw-Hill, New York, 1968).

Appendix

In this appendix, we solve the coupled partial differential equation eq. (22) with the boundary conditions of eqs. (23)–(25). Hereafter, we omit the subscript i for simplicity.

We define the Laplace transformations of $G(x, t)$ and $N(x, t)$ as

$$g(x, s) = \int_0^\infty G(x, t)e^{-st} dt \quad (37)$$

$$n(x, s) = \int_0^\infty N(x, t)e^{-st} dt \quad (38)$$

Then, eq. (22) becomes

$$\begin{aligned} v \frac{\partial g(x, s)}{\partial x} &= -(s + \tilde{k})g(x, s) + kn(x, s) + G(x, 0), \\ (s + k)n(x, s) &= \tilde{k}g(x, s). \end{aligned} \quad (39)$$

We can easily solve this coupled differential equation as

$$\begin{aligned} g(x, s) &= G\{s^{-1} - h^{-1}(s)\}e^{-h(s)x/v} + G(x, 0)h^{-1}(s), \\ n(x, s) &= \frac{\tilde{k}}{s + k}g(x, s), \end{aligned} \quad (40)$$

where

$$h(s) = s + \tilde{k} - \frac{\tilde{k}k}{s + k}. \quad (41)$$

Integrating $g(x, s)$ and $n(x, s)$ with respect to x from 0 to L , we have

$$\begin{aligned} g(s) &= \int_0^L g(x, s) ds \\ &= -G \frac{\tilde{k}}{(\tilde{k} + k)^2} v \left\{ \frac{k}{s^2} - \frac{\tilde{k}}{(s + \tilde{k} + k)^2} + \frac{\tilde{k} - k}{s(s + \tilde{k} + k)} \right\} \left\{ e^{-h(s)L/v} - 1 \right\} \\ &\quad + G \frac{1}{\tilde{k} + k} \left\{ \frac{k}{s} - \frac{\tilde{k}}{s + \tilde{k} + k} \right\}, \end{aligned} \quad (42)$$

$$\begin{aligned} n(s) &= \int_0^L n(x, s) ds \\ &= -G \frac{\tilde{k}^2}{(\tilde{k} + k)^2} v \left\{ \frac{1}{s^2} - \frac{1}{(s + \tilde{k} + k)^2} + \frac{2}{s(s + \tilde{k} + k)} \right\} \left\{ e^{-h(s)L/v} - 1 \right\} \end{aligned}$$

$$+G \frac{\tilde{k}}{\tilde{k}+k} \left\{ \frac{1}{s} - \frac{1}{s+\tilde{k}+k} \right\}. \quad (43)$$

Finally, expanding the exponential function in the Taylor series, we carry out the anti-Laplace transformation on each term in the series and obtain

$$G_i(t) = -G_i \frac{\tilde{k}_i}{(\tilde{k}_i + k_i)} \left[-L(\tilde{k}_i + k_i) \left\{ 1 - e^{-(\tilde{k}_i + k_i)t} \right\} - L \left(k_i e^{-k_i L/v} - \tilde{k}_i e^{\tilde{k}_i L/v} \right) e^{-k_i t} + v \frac{\tilde{k}_i - k_i}{\tilde{k}_i + k_i} \left(e^{-k_i L/v} - e^{\tilde{k}_i L/v} \right) e^{-k_i t} + \frac{2v}{k_i} \frac{\tilde{k}_i - k_i}{\tilde{k}_i + k_i} e^{\tilde{k}_i L/v} H_i(t) e^{-k_i t} \right] + G_i \frac{1}{\tilde{k}_i + k_i} \left\{ k_i + \tilde{k}_i e^{-(\tilde{k}_i + k_i)t} \right\}, \quad (44)$$

$$N_i(t) = -G_i \frac{\tilde{k}_i^2}{(\tilde{k}_i + k_i)^2} \left[-L \left\{ 1 + \frac{\tilde{k}_i}{k_i} + \left(1 + \frac{k_i}{k_i} \right) e^{-(\tilde{k}_i + k_i)t} \right\} + L \left(\frac{k_i}{\tilde{k}_i} e^{-k_i L/v} + \frac{\tilde{k}_i}{k_i} e^{\tilde{k}_i L/v} \right) e^{-k_i t} - \frac{2v}{\tilde{k}_i + k_i} \left(e^{-\tilde{k}_i L/v} - e^{k_i L/v} \right) e^{-k_i t} \right] + G_i \frac{\tilde{k}_i}{\tilde{k}_i + k_i} \left\{ 1 - e^{-(\tilde{k}_i + k_i)t} \right\}, \quad (45)$$

where

$$H_i(t) = \sum_{n=2}^{\infty} \frac{1}{n!(n-1)!} \left(\tilde{k}_i k_i \frac{L}{v} \right)^n \left(t - \frac{L}{v} \right)^{n-1}. \quad (46)$$